

## The Dehydration of Boehmite, $\gamma$ -AlOOH, to $\gamma$ -Al<sub>2</sub>O<sub>3</sub>

S. J. WILSON

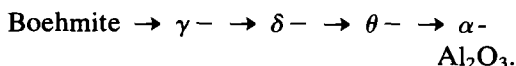
*Department of Mineralogy and Petrology, University of Cambridge,  
Cambridge, England*

Received August 25, 1978; in revised form January 15, 1979

Electron microscopic observations of microstructure, together with studies of the evolution of X-ray and electron diffraction patterns, have been used to provide mechanistic information on the dehydration of boehmite to  $\gamma$ -Al<sub>2</sub>O<sub>3</sub>. Firing boehmite in air at 400°C produces slow development of a fine, lamellar, porous microstructure, oriented parallel to (001)<sub>γ</sub>, the dimensions of which are consistent with the loss of one-quarter of the oxygen atoms of the boehmite lattice. The mechanism proposed for the dehydration is controlled by diffusion in a direction determined by the hydrogen bond chains in the boehmite structure and involves counter migration of the Al cations and protons with crystallographic formation of voids in a coherent cubic close-packed matrix. Final reorganization to give the spinel structure of  $\gamma$ -Al<sub>2</sub>O<sub>3</sub> is suggested to involve gradual filling of the tetrahedral cation sites.

### Introduction

Previous studies of the dehydration of boehmite ( $\gamma$ -AlOOH) (1, 2) have shown that a series of metastable alumina phases are produced before final conversion to the thermodynamically stable phase, corundum ( $\alpha$ -Al<sub>2</sub>O<sub>3</sub>):



The temperatures at which these transitions have been observed are somewhat variable, apparently dependent on the crystallinity and previous history of the boehmite and on the conditions of heat treatment (3). The transformations in this sequence are topotactic at least as far as  $\delta$ -Al<sub>2</sub>O<sub>3</sub> (2) and probably also to  $\theta$ -Al<sub>2</sub>O<sub>3</sub> (4).

Boehmite has the orthorhombic layered structure shown in Fig. 1a (5, 6). Within each layer the oxygen packing is cubic close-packed although the overall structure is not close-packed. The hydroxyl groups are on the

surfaces of the layers, the arrangement of which suggests that the layers are held together by zigzag chains of hydrogen bonds running parallel to the boehmite *a* axis with O-H-O distances of about 2.70 Å. The existence of such chains was found to be necessary to explain the infrared spectrum of boehmite (7). A neutron diffraction study of the isostructural  $\gamma$ -FeOOH showed that the hydrogen bonds are symmetrical with the protons midway between oxygen atoms (8). That this is also the case for boehmite is suggested by the infrared work of Stegmann (9); however, in the light of the established mobility of protons in boehmite (10-12) this may be regarded as the mean position of the protons.

$\gamma$ -Al<sub>2</sub>O<sub>3</sub> has a defect spinel structure with a tetragonal distortion (2, 4) and thus is characterized by a close-packed cubic anion lattice. The positions of the cation vacancies have not, however, been established. The structures of  $\delta$ - and  $\theta$ -Al<sub>2</sub>O<sub>3</sub> are also very similar to that of spinel (2, 13, 14).

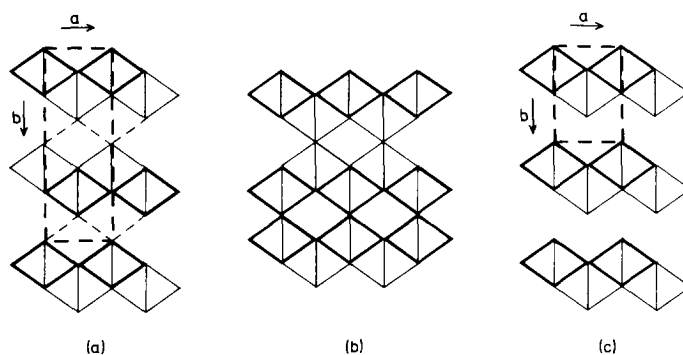
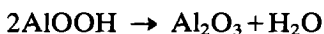


FIG. 1. Idealized structures of (a) boehmite, (b) collapsed boehmite (*ccp* lattice), and (c) FeOCl.

The pseudomorphosis relationships for the topotactic dehydration of boehmite to  $\gamma$ - $\text{Al}_2\text{O}_3$  are (2, 4) (using boehmite parameters from Ref. (15)):

$$\begin{aligned} a_{\text{Bo}} & 3.700 \text{ \AA} \rightarrow [001]_{\gamma} \\ b_{\text{Bo}} & 12.227 \text{ \AA} \rightarrow [110]_{\gamma} \\ c_{\text{Bo}} & 2.868 \text{ \AA} \rightarrow [1\bar{1}0]_{\gamma} \end{aligned}$$

The stoichiometry of the reaction



indicates that one-quarter of the boehmite oxygen lattice is lost during the decomposition. For the dehydration of hydroxide species with layered structures, two general types of mechanism have been suggested. The most widely proposed mechanism for layered hydroxides, based mainly on crystallographic considerations of the topotactic relationships observed, is one which involves elimination of  $\text{H}_2\text{O}$  by an internal condensation of protons and hydroxyl groups between the layers followed by collapse of the layered structure. Such a mechanism has been assumed for the dehydrations of  $\gamma$ - $\text{AlOOH}$  (2, 4, 16),  $\gamma$ - $\text{FeOOH}$  (17, 18),  $\text{Co}(\text{OH})_2$  (19), and  $\text{Cd}(\text{OH})_2$  (20). In the case of boehmite the initial product of such a collapse mechanism would be the cubic close-packed lattice illustrated in Fig. 1b. The development of a porous microstructure observed during the dehydrations of

$\text{Co}(\text{OH})_2$  and  $\text{Cd}(\text{OH})_2$  was attributed to the formation of cracks due to the strains set up in the lattice during the process of collapse.

An alternative view of the dehydration process is that suggested by Ball and Taylor (21) for the dehydration of brucite,  $\text{Mg}(\text{OH})_2$ . This involves countermigration of Mg cations and protons and elimination of  $\text{H}_2\text{O}$ , resulting in the formation of regions of MgO separated by voids. Under this mechanism the development of a porous microstructure would be an integral part of the reaction mechanism.

A previous study (22) has followed the development of microstructure during the dehydration of boehmite. The aim of the present work is to examine the mechanistic information which may be derived from studies of the evolution of X-ray and electron diffraction patterns, and from the nature of the microstructure produced, during the low-temperature dehydration of boehmite to  $\gamma$ - $\text{Al}_2\text{O}_3$ .

## Experimental

The synthetic boehmite used in this study was CERA hydrate supplied by the British Aluminium Company Ltd. which had a maximum crystal size of about  $5 \mu\text{m}$ . Material for examination was furnace-fired isothermally in air in platinum crucibles. X-Ray characterization was performed using a

Philips powder diffractometer with  $\text{CuK}\alpha$  radiation.

Samples for electron microscopy were prepared by crushing, dispersing in alcohol, and depositing on perforated carbon films on copper support grids. Transmission electron microscopy was performed on a Siemens 102 instrument equipped with a double-tilting stage and operated at 100 kV.

## Results

The well-crystallized boehmite used in this study had the form of thin plates with a basal plane parallel to the layers in the boehmite structure. The easy cleavage parallel to this plane resulted in crushed grains producing fragments with predominantly  $(010)_{\text{Bo}}/(110)_{\gamma}$  surfaces. The electron microscopic observations reported here relate to such fragments.

The evolution of electron diffraction patterns during the transformation of boehmite to  $\gamma\text{-Al}_2\text{O}_3$  was studied by beam heating fragments of boehmite previously unfired or else furnace-fired at  $400^\circ\text{C}$  for only a few hours. Heating boehmite in the electron beam results in a fast dehydration process, due to the high vacuum, and the production of a characteristic fine random porous microstructure (22). A typical sequence of diffraction patterns is shown in Fig. 2. The original boehmite  $[010]$  pattern is

developed first by the appearance of disallowed reflections. This is followed by the gradual appearance of the characteristic spinel reflections until finally a well-developed coherent  $\gamma\text{-Al}_2\text{O}_3$   $[110]$  pattern is produced. There is evidence in the intermediate patterns (Figs. 2b and c) of the small expansion of  $a_{\text{Bo}}$  ( $\sim 6\%$ ) and contraction of  $c_{\text{Bo}}$  ( $\sim 2\%$ ) necessary for the formation of the  $\gamma\text{-Al}_2\text{O}_3$  lattice.

In samples of boehmite furnace-fired at  $400^\circ\text{C}$ , the dehydration process is accompanied by the slow development on the  $(010)_{\text{Bo}}$  surfaces of a characteristic porous microstructure with a growth direction perpendicular to the crystal surface (22). After firing for 1 week at  $400^\circ\text{C}$  this microstructure is well developed (see Fig. 3). At this stage X-ray powder studies indicate that dehydration is 80–90% complete and that the  $\gamma\text{-Al}_2\text{O}_3$  produced is tetragonal with  $a = 7.96 \text{ \AA}$ ,  $c = 7.81 \text{ \AA}$ . The microstructure of Fig. 3a shows the traces of intersection of a fine pore system with the crystal surface. The high contrast suggests that we are looking directly down a series of sheet-like pores parallel to  $(001)_{\gamma}$ . Although there is evidence of crosslinking between adjacent pores and of deviations from linearity the regularity of orientation and of the spacing of the pores is nevertheless remarkable. The pore spacing is of the order of  $35\text{--}40 \text{ \AA}$  while the average pore width is about  $8 \text{ \AA}$ . In Fig. 3b  $(111)_{\gamma}$

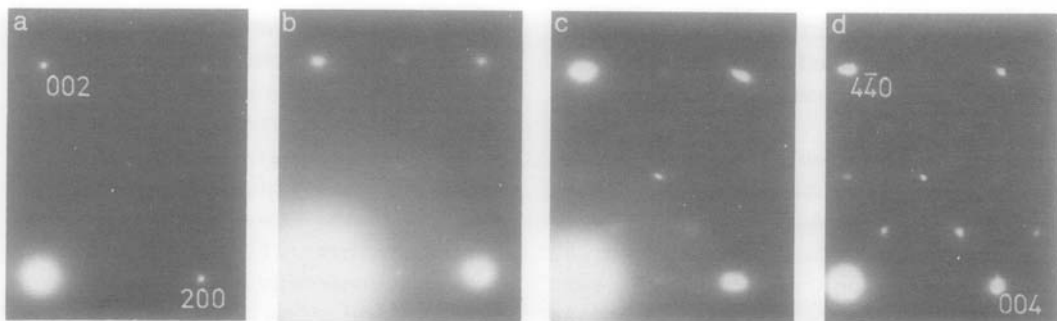


FIG. 2. Typical electron diffraction pattern sequence for electron beam-induced dehydration of boehmite, from (a)  $[010]_{\text{Bo}}$  to (d)  $[110]_{\gamma}$ .

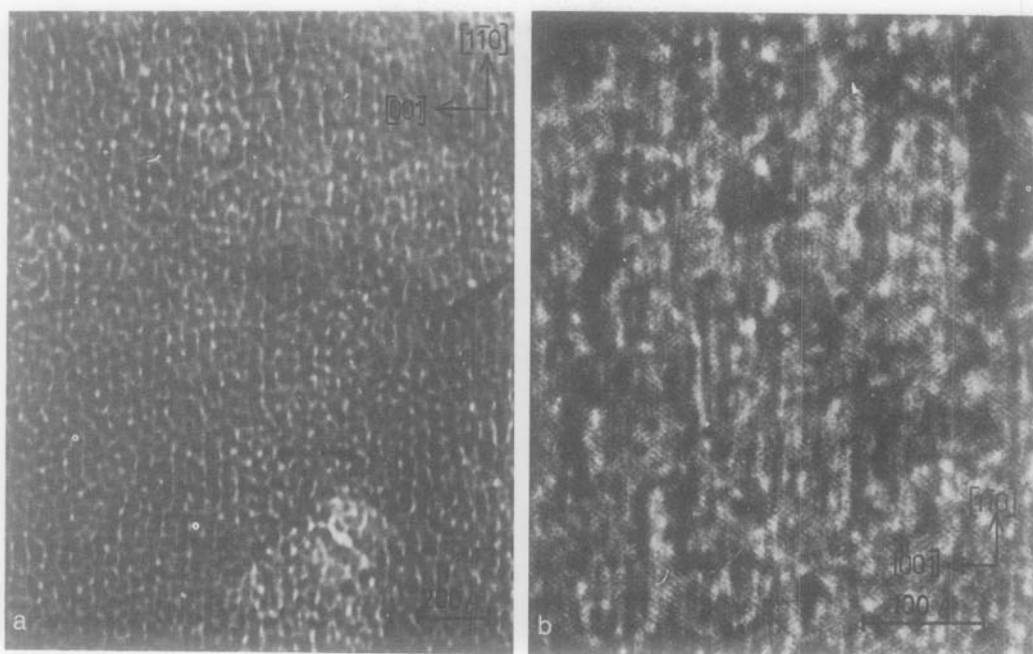


FIG. 3. (a) Lamellar porous microstructure produced by firing boehmite in air at 400°C.  $[110]_{\gamma}$  orientation. (b) Resolution of  $(111)_{\gamma}$  lattice fringes.

lattice fringes with a spacing of 4.6 Å are resolved in the regions between the pores. These fringes are hardly disrupted by the presence of the pores, showing the coherence of the  $\gamma\text{-Al}_2\text{O}_3$  lattice. There is some evidence though of slight changes in direction of the lattice fringes across the pores which might indicate slight angular misorientation of blocks of  $\gamma\text{-Al}_2\text{O}_3$ . However, this effect might also be caused by phase changes due to irregular variations in crystal thickness, which are to be expected in a porous material, or to variations in the degree of deviation from the Bragg angle or the degree of defocus (23).

Electron diffraction patterns from fragments showing this lamellar porous microstructure are characteristic of well-developed coherent  $\gamma\text{-Al}_2\text{O}_3$ . Figure 4a shows the commonly observed  $[110]_{\gamma}$  zone which exhibits prominent streaking along the  $c_{\gamma}^*$  direction. Structure factor calculations based on the ideal cubic spinel lattice

indicate that the most strongly streaked reflections are those with contributions only from cation positions and not from the oxygen sublattice. More specifically the streaking in the  $[110]_{\gamma}$  pattern is associated with the contribution to the intensity from the tetrahedral cation positions, since reflections due only to the octahedral cation sites and the oxygen sublattice, such as  $2\bar{2}2$ , are the sharpest. By tilting crystal fragments other  $\gamma\text{-Al}_2\text{O}_3$  diffraction patterns also exhibiting streaking effects were obtained. These orientations in the essentially pseudocubic  $\gamma\text{-Al}_2\text{O}_3$  reciprocal lattice were indexed with regard to trace analysis of the  $(001)_{\gamma}$  pore system and to analysis of the apparent crystal shapes. The identity of the strongly streaked reflections is not, however, the same in all orientations. In the  $[21\bar{1}]_{\gamma}$  zone of Fig. 4b the streaking is apparently again associated with the tetrahedral cation sites, with reflections such as  $2\bar{2}2$  being the sharpest. However, in the  $[011]_{\gamma}$  zone of Fig. 4c the streaking is

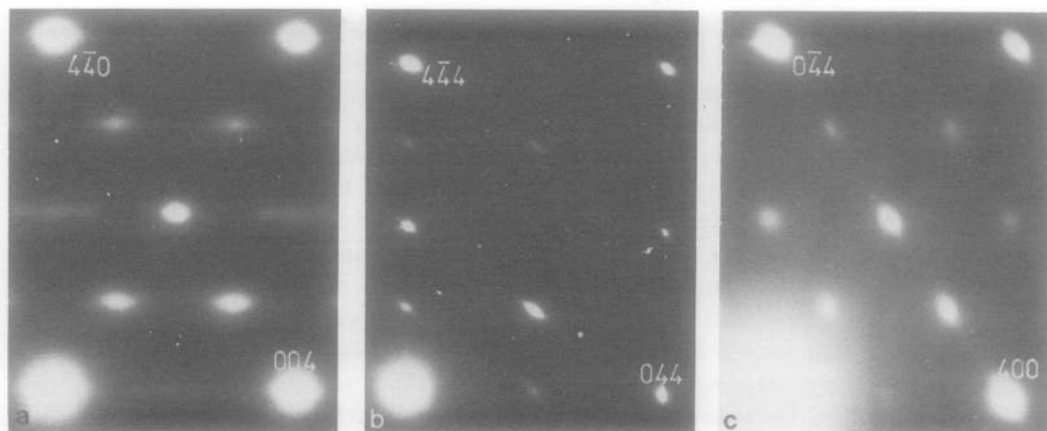


FIG. 4. Streaking effects in electron diffraction patterns from furnace-fired boehmite fragments exhibiting the lamellar porous microstructure. (a)  $[110]$ , (b)  $[21\bar{1}]$ , and (c)  $[011]$   $\gamma$ - $\text{Al}_2\text{O}_3$  zones.

associated with the contribution to the intensity from the octahedral cation sites and/or the oxygen sublattice, since reflections such as  $0\bar{2}2$ , which has a contribution only from the tetrahedral positions, are now the least streaked. In all orientations, though, the streaking observed in the diffraction patterns is in a direction perpendicular to the trace of the pore system. X-Ray powder patterns from  $\gamma$ - $\text{Al}_2\text{O}_3$  material with this lamellar microstructure exhibit broad reflections, as found also for  $\gamma$ - $\text{Fe}_2\text{O}_3$  produced by dehydration of  $\gamma$ - $\text{FeOOH}$  (18), but here again reflections with strong contributions from cation positions are broadened most significantly. The degree of X-ray line broadening is consistent with the pore spacing observed in electron micrographs.

In samples fired for periods longer than 1 week at  $400^\circ\text{C}$  or for short times at  $600^\circ\text{C}$  the lamellar porous microstructure is still well developed but is starting to appear more complex, presumably due to some sintering process. These higher temperature treatments also give rise to the onset of the transformation of  $\gamma$ - to  $\delta$ - $\text{Al}_2\text{O}_3$ . For samples in which the degree of transformation to  $\delta$ - $\text{Al}_2\text{O}_3$  is insignificant, there is an interesting evolution of the lattice parameters of  $\gamma$ - $\text{Al}_2\text{O}_3$  (Table I). The degree of tetragonal distortion of the spinel lattice of  $\gamma$ - $\text{Al}_2\text{O}_3$  decreases with an increase in the time or temperature of heat treatment. This gradual development of a nearly cubic phase is followed by a further increase in the distortion as the transformation to tetragonal  $\delta$ - $\text{Al}_2\text{O}_3$  becomes important.

TABLE I  
EVOLUTION OF  $\gamma$ - $\text{Al}_2\text{O}_3$  LATTICE PARAMETERS

	Heat treatment of boehmite ( $^\circ\text{C}$ )					
	400 (1 wk)	400 (8 wk)	600 (1 d)	400 (1 d) 600 (1 d)	600 (1 wk)	600 (8 wk)
$c/a$ for $\gamma$ - $\text{Al}_2\text{O}_3$	0.981	0.987	0.988	0.993	0.990	0.988

## Discussion

The microstructure produced during the dehydration of boehmite and described here has similarities to that observed during the dehydration of the isostructural  $\gamma$ -FeOOH (18). The interpretation put forward in this case was one involving collapse of the lattice, producing strings of spinel structure running through an undecomposed  $\gamma$ -FeOOH matrix. However, one should not expect to observe such high contrast between two such similar phases which, because of the topology of the transformation, should both reflect strongly in the same orientation. Recent work on the development of microstructure during the dehydration of boehmite (22) has established that the texture observed is in fact of a porous nature, and that the interpretation of the microstructure in terms of lamellar pores agrees well with measurements of surface area by adsorption methods. Further evidence is provided by Fig. 3b which shows (111)-spinel lattice fringes in the regions between the pores.

Nevertheless, as a general mechanism for the dehydration of layered hydroxides, one involving collapse across the layers with elimination of  $H_2O$  between layers by an internal condensation of protons and hydroxyl groups has been found attractive. Indeed for the boehmite structure such a mechanism seems an obvious possibility from a structural point of view because of the production thereby of the cubic close-packed framework of the spinel structure (Fig. 1b). However, the dehydration of boehmite via a collapse mechanism does not require the formation of pores. It has been suggested for other systems (19, 20) that strains set up in the crystal during a collapse process might produce fragmentation, resulting in an apparently porous texture and slight misorientations between the adjacent oxide blocks thus formed. However, the results of the present study of the dehydration of boehmite, in particular the regularity of the

orientation and spacing of the lamellar porous microstructure, the coherence of the  $\gamma$ - $Al_2O_3$  electron diffraction patterns, and the coherence of the (111) $_{\gamma}$  lattice fringes across the pores, suggest that in this case the formation of the pore system is crystallographic and a necessary feature of the reaction mechanism. Furthermore, dehydration of boehmite via collapse would require considerable shrinkage (31%) of the boehmite  $b$  parameter, 12.227 Å, to 8.44 Å ( $\frac{2}{3}d_{110}$ ) in  $\gamma$ - $Al_2O_3$ . Dilatometric data reported for crystalline boehmite (24) show that no shrinkage is observed below 1200°C.

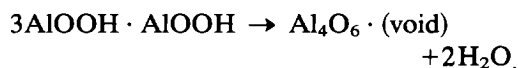
It is perhaps not possible to rule out completely the possibility of a collapse mechanism for the dehydration of boehmite since, in orientations perpendicular to  $b_{Bo}$ , pores have been observed parallel to the layers in the boehmite structure (22). If the process of dehydration can be assumed to advance from the surfaces of crystals it is not unreasonable that the mechanism may vary with the identity of the crystal surface. However, in the thin platy crystalline boehmite studied here, (010) $_{Bo}$  faces predominate and the lamellar microstructure is developed over a time scale shown by X-ray work to be consistent with that for loss of  $H_2O$ , so that the observed microstructure must be characteristic of an important mechanism for the dehydration process.

The appearance of the (001) $_{\gamma}$  pore system, together with the fact that its direction of growth is perpendicular to the (110) $_{\gamma}$  surface, suggests, by analogy with metallurgical eutectic and eutectoid lamellar microstructures, that the dehydration mechanism is controlled by a diffusion process perpendicular to the pores, i.e., along [001] $_{\gamma}$ . The fact that when dehydration is performed *in situ* in the electron microscope, under conditions of temperature and pressure which promote a much faster reaction, the porous microstructure produced is even finer in scale (22), lends further support to the idea of diffusion control of the

mechanism. The  $[001]_y$  direction in the boehmite structure is that followed by the hydrogen bond chains which might thus provide a path for proton diffusion. There is ample evidence that in boehmite the protons are indeed mobile (10–12). This mobility increases with temperature and is considerable at temperatures below the onset of dehydration. A proton tunneling process along the hydrogen bond chains has been suggested as the source of the mobility (10).

Thus a dehydration mechanism was sought which would account for the observed microstructure, involving counter migration of protons and Al cations, similar to that suggested for  $Mg(OH)_2$  by Ball and Taylor (21) but with the added constraint that the direction of diffusion should be governed by the hydrogen bond chain in the boehmite structure. The mechanism proposed is illustrated in Fig. 5. Protons are lost from between the boehmite layers by a diffusion process along the hydrogen bond chains and the interlayer sites thus created are occupied by counterdiffusing Al cations. A small degree of movement of the boehmite layers is necessary for these sites to become octahedral and for the overall oxygen lattice to become *fcc*. The elimination of  $H_2O$  is due to the abstraction by the protons of oxygen anions and hydroxyl groups from the region of the now-vacant Al sites. This results in the formation of regions of void which appear as pores, the surfaces of which will presumably be highly protonated. One interlayer site is

created for every proton lost and the stoichiometry of the overall dehydration requires that one-third of these sites should be filled by Al cations. On the basis of this mechanism the overall loss of one-quarter of the oxygen anions from the boehmite lattice implies that the pore volume should occupy one-quarter of the original crystal volume. The stoichiometry of the proposed diffusion reaction may be formulated as



The formation of the spinel lattice of  $\gamma\text{-Al}_2\text{O}_3$  must be accomplished by final reorganization of the Al cation positions.

The mechanism as described above produces a coherent skeleton of  $\gamma\text{-Al}_2\text{O}_3$  based on the original boehmite lattice and intersected by pores which should be perpendicular to the direction of diffusion. This is entirely consistent with the observed fine lamellar  $(001)_\gamma$  pore system and the coherence of  $\gamma\text{-Al}_2\text{O}_3$  electron diffraction patterns and lattice fringes. The mechanism proposed undoubtedly offers vast opportunities for mistakes to be made and this accounts for the slight deviations from linearity and the crosslinking of pores observed. In general, though, the regularity of orientation and spacing of the observed microstructure is remarkable.

As stated above, slight movement of the boehmite layers is necessary for the formation of octahedral interlayer sites and a cubic close-packed oxygen lattice. The relative movement of layers required is approximately  $c_{Bo}/2$  ( $1.43 \text{ \AA}$ ) which is much less than that ( $2.70 \text{ \AA}$ ) required for the collapse mechanism. This  $c/2$  movement produces an arrangement of the layers which is similar to that found in the structure of  $FeOCl$  (25) (Fig. 1c) in which the oxygen and chlorine anions are approximately cubic close-packed.  $AlOCl$  was originally thought to be isostructural with  $FeOCl$  (26) but was later shown (27) to have the  $GaOCl$  structure (28)

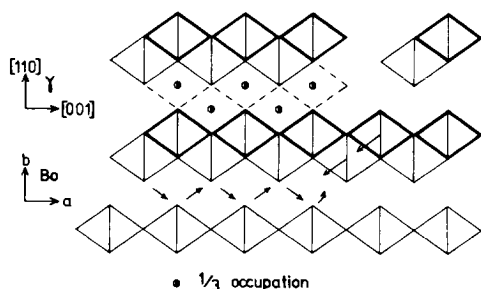


FIG. 5. Schematic illustration of the proposed mechanism for the dehydration of boehmite.

with tetrahedrally coordinated Al cations. In the structures of FeOCl and  $\gamma$ -FeOOH (isostructural with boehmite) the arrangement of octahedra within layers is identical but the stacking of the layers differs. It seems that the formation of the hydrogen bond chains is responsible for the particular arrangement found in the boehmite structure. Thus it is quite conceivable that during the dehydration of boehmite, loss of protons should be accompanied by a  $c/2$  shift and the production of the FeOCl layer arrangement.

Diffusion of Al cations into the octahedral interlayer sites in this FeOCl-type structure suggests that a defect NaCl-type intermediate is formed before cation reorganization finally produces the spinel structure. Evidence that this might be the case is provided by the electron diffraction pattern sequence of Fig. 2, in which evolution of the lattice parameters toward those of the *fcc* spinel lattice is evident before the characteristic spinel reflections appear. The additional disallowed boehmite reflections which appear in Fig. 2b are also compatible with a defect NaCl structure in which only octahedral sites are occupied.

The idea that reorganization of the cation distribution in a defect NaCl-type intermediate might lead ultimately to the spinel structure suggests that initially in the defect  $\text{Al}_2\text{O}_3$  spinel the vacancies are on tetrahedral sites. Evidence in the literature on the positions of vacancies in  $\gamma$ - $\text{Al}_2\text{O}_3$  is not available, although Leonard *et al.* (29) have demonstrated for a series of heat-treated alumina gels that radial electron density distribution functions can provide information on cation distributions. Saalfeld (4) considered that vacancies in  $\gamma$ - $\text{Al}_2\text{O}_3$  are probably on tetrahedral sites and also proposed a defect NaCl structure as an intermediate in the dehydration of boehmite via a collapse mechanism. He suggested further that the tetragonal distortion of  $\gamma$ - $\text{Al}_2\text{O}_3$  and the shortened  $c$  axis are due to a cation distribution in which octahedral sites are pre-

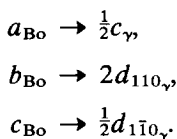
dominantly occupied. Thus the decrease in tetragonal distortion with increase in the time or temperature of heat treatment observed in the present study may provide evidence of a gradual reorganization of cations in  $\gamma$ - $\text{Al}_2\text{O}_3$ , with an increase in the number of tetrahedral sites occupied accompanied by an increase in octahedral vacancies. There appears then to be a trend toward the replacement of tetrahedral by octahedral vacancies during heat treatment of  $\gamma$ - $\text{Al}_2\text{O}_3$  formed by the dehydration of boehmite. Certainly there is evidence that in  $\gamma$ - $\text{Fe}_2\text{O}_3$ , which is probably isostructural with  $\delta$ - $\text{Al}_2\text{O}_3$  (30), all the vacancies are on octahedral sites (31, 32).

Lippens and de Boer (2) observed streaking of  $[110]_\gamma$  electron diffraction patterns similar to that found in the present work (Fig. 4a). They concluded from structure factor considerations that this revealed considerable disorder in the occupation of the tetrahedral sites. However, Fig. 4c shows that in some orientations the streaking is associated with the octahedral site or oxygen sublattice contribution to the intensity. In all orientations the direction of streaking was observed to be perpendicular to the trace of the pore system. Furthermore  $[110]$  patterns from  $\gamma$ - $\text{Al}_2\text{O}_3$ , produced by beam heating and having a random porous microstructure, show no streaking effects (Fig. 2d). Thus the observed streaking is due to the strict directionality of the lamellar porous microstructure, though why the reflection type affected most strongly should vary with orientation is not clear.

One final test of the proposed mechanism can be applied directly to the observed microstructure. The idealized mechanism requires that the pore volume should be one-quarter of the original crystal volume, and, furthermore, that the pores emerging at the  $(110)_\gamma$  surface should account for one-quarter of the area of that surface. In fact the 6% expansion of  $a_{D0}$  necessary for production of the  $\gamma$ - $\text{Al}_2\text{O}_3$  lattice will be taken up by the

pores, reducing their proportion of the surface area to about 0.21. The observed pore width ( $\sim 8 \text{ \AA}$ ) and repeat distance (35–40  $\text{\AA}$ ) are thus consistent with this. It should be noted that with the scale of the microstructure at the level of about 40  $\text{\AA}$ , the width of the lamellae of  $\gamma\text{-Al}_2\text{O}_3$  (of the order of 27–32  $\text{\AA}$ ) must in fact be integral multiples of half the octahedron length in the [001] direction of the  $\gamma\text{-Al}_2\text{O}_3$  structure (1.99  $\text{\AA}$ ).

On the basis of the proposed mechanism the pseudomorphosis relationships for the dehydration of boehmite to  $\gamma\text{-Al}_2\text{O}_3$  become:



### Acknowledgments

Helpful discussions with Dr. J. D. C. McConnell and the receipt of an award under the ICI Joint Research Scheme are gratefully acknowledged.

### References

1. H. C. STUMPF, A. S. RUSSELL, J. W. NEWSOME, AND C. M. TUCKER, *Ind. Eng. Chem.* **42**, 1398 (1950).
2. B. C. LIPPENS AND J. H. DE BOER, *Acta Crystallogr.* **17**, 1312 (1964).
3. B. C. LIPPENS, Thesis, Delft (1961).
4. H. SAALFELD, *Clay Miner. Bull.* **3**, 249 (1958).
5. W. O. MILLIGAN AND J. L. MCATEE, *J. Phys. Chem.* **60**, 273 (1956).
6. H. BOSMANS, Thesis, Leuven (1966).
7. K. A. WICKERSHEIM AND G. K. KORPI, *J. Chem. Phys.* **42**, 579 (1965).
8. A. OLES, A. SZYTULA, AND A. WANIC, *Phys. Status Solidi* **41**, 173 (1970).
9. M. C. STEGMANN, D. VIVIEN, AND C. MAZIERES, *Spectrochim. Acta Part A* **29**, 1653 (1973).
10. J. J. FRIPIAT, H. BOSMANS, AND P. G. ROUXHET, *J. Phys. Chem.* **71**, 1097 (1967).
11. A. MATA ARJONA AND J. J. FRIPIAT, *Trans. Faraday Soc.* **63**, 2936 (1967).
12. J. J. FRIPIAT AND R. TOUILLAU, *Trans. Faraday Soc.* **65**, 1236 (1969).
13. J. A. KOHN, G. KATZ, AND J. D. BRODER, *Amer. Mineral.* **42**, 398 (1957).
14. G. KATZ, A. W. NICOL, AND R. ROY, *Z. Kristallogr.* **130**, 388 (1969).
15. H. E. SWANSON AND R. K. FUYAT, *Nat. Bur. Stand. U.S. Circ.* **539** **3**, 38 (1953).
16. K. SASVARI AND A. ZALAI, *Acta Geol. Acad. Sci. Hung.* **4**, 415 (1957).
17. T. TAKADA, M. KIYAMA, AND S. SHIMIZU, *Bull. Inst. Chem. Res. Kyoto Univ.* **42**, 505 (1964).
18. R. GIOVANOLI AND R. BRUTSCH, *Chimia* **28**, 188 (1974).
19. M. FIGLARZ, J. GUENOT, AND F. FIEVET-VINCENT, *J. Mater. Sci.* **11**, 2267 (1976).
20. J. C. NIEPCE, M. T. MESNIER, AND D. LOUER, *J. Solid State Chem.* **22**, 341 (1977).
21. M. C. BALL AND H. F. W. TAYLOR, *Mineral. Mag.* **32**, 754 (1961).
22. S. J. WILSON, *Mineral. Mag.*, in press.
23. J. M. COWLEY, *Acta Crystallogr.* **12**, 367 (1959).
24. P. A. BADKAR, J. E. BAILEY, AND H. A. BARKER, in "Materials Science Research" (G. C. Kuczynski, Ed.), Vol. 6, p. 311, Plenum, New York (1973).
25. M. D. LIND, *Acta Crystallogr. Sect. B* **26**, 1058 (1970).
26. J. ROUXEL, *C.R. Acad. Sci. Paris* **248**, 810 (1959).
27. P. HAGENMULLER, J. ROUXEL, J. DAVID, A. COLIN, AND B. LE NEINDRE, *Z. Anorg. Allg. Chem.* **323**, 1 (1963).
28. A. HARDY AND A. M. HARDY, *C.R. Acad. Sci. Paris* **256**, 3477 (1963).
29. A. J. LEONARD, F. VAN CAUWELAERT, AND J. J. FRIPIAT, *J. Phys. Chem.* **71**, 695 (1967).
30. G. W. VAN OOSTERHOUT AND C. J. M. ROOIJMAN, *Nature* **181**, 44 (1958).
31. R. J. ARMSTRONG, A. H. MORRISH, AND G. A. SAWATZKY, *Phys. Lett.* **23**, 414 (1966).
32. B. GILLOT, F. BOUTON, J. F. FERRIOT, F. CHASAGNEUX, AND A. ROUSSET, *J. Solid State Chem.* **21**, 375 (1977).